Supplemental Information

for

Enabling method to design versatile biomaterial systems from colloidal building blocks

Shalini Saxena,[1,2*] L. Andrew Lyon[3*]

[1]School of Materials Science and Engineering, Georgia Institute of Technology, Atlanta, GA 30332, USA

[2]Petit Institute for Biosciences and Bioengineering, Georgia Institute of Technology, Atlanta, GA 30332, USA

[3]Schmid College of Science and Technology, Chapman University, Orange, CA 92866, USA

*Corresponding Authors
Shalini Saxena
Email: ssaxena30@gatech.edu

L. Andrew Lyon
Email: lyon@chapman.edu
Telephone: 714-997-6930
Fax: 714-532-6048

Scheme S1. (A) Depiction of the physical restrictions of the microgel assembly caused by the EDC/NHS coupling. (B) Depiction of the EDC/NHS carbodiimide coupling chemistry between the microgel (M) and polycation (P).

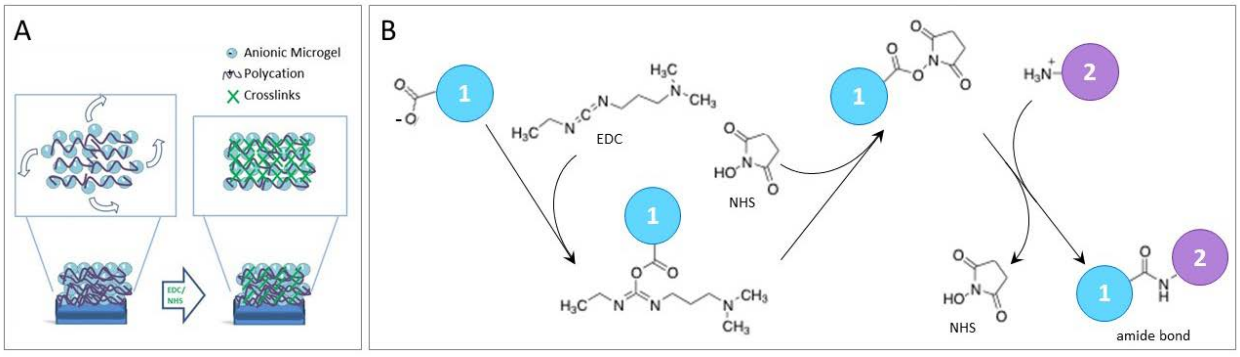

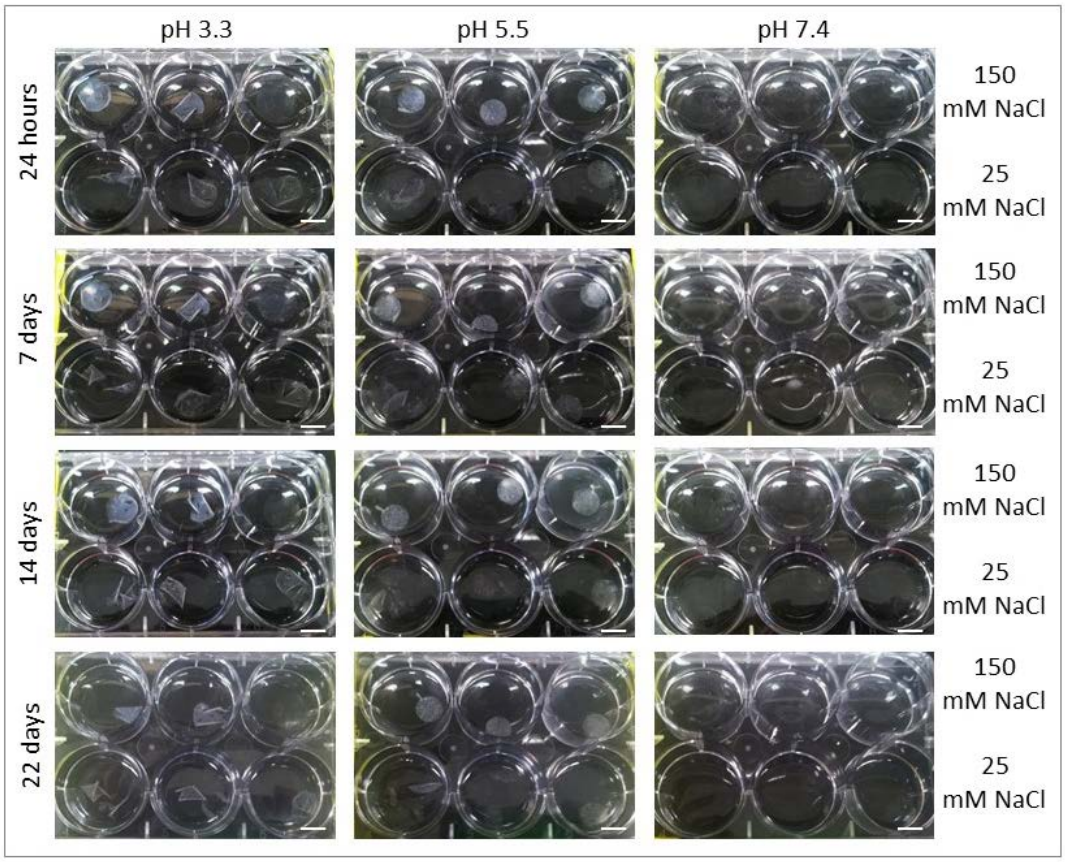

Figure S1. Characterization of microgel film swelling. Microgel films were prepared using the single-step method and left until dry. Films were then solvated in six buffers for several weeks to observe detachment. Buffer conditions included a high salt concentration (25 mM NaCl) and a low salt concentration (150 mM NaCl) for formate buffer (pH 3.3), MES buffer (pH 5.5), and PBS (pH 7.4). Scale bars represent 10 mm.

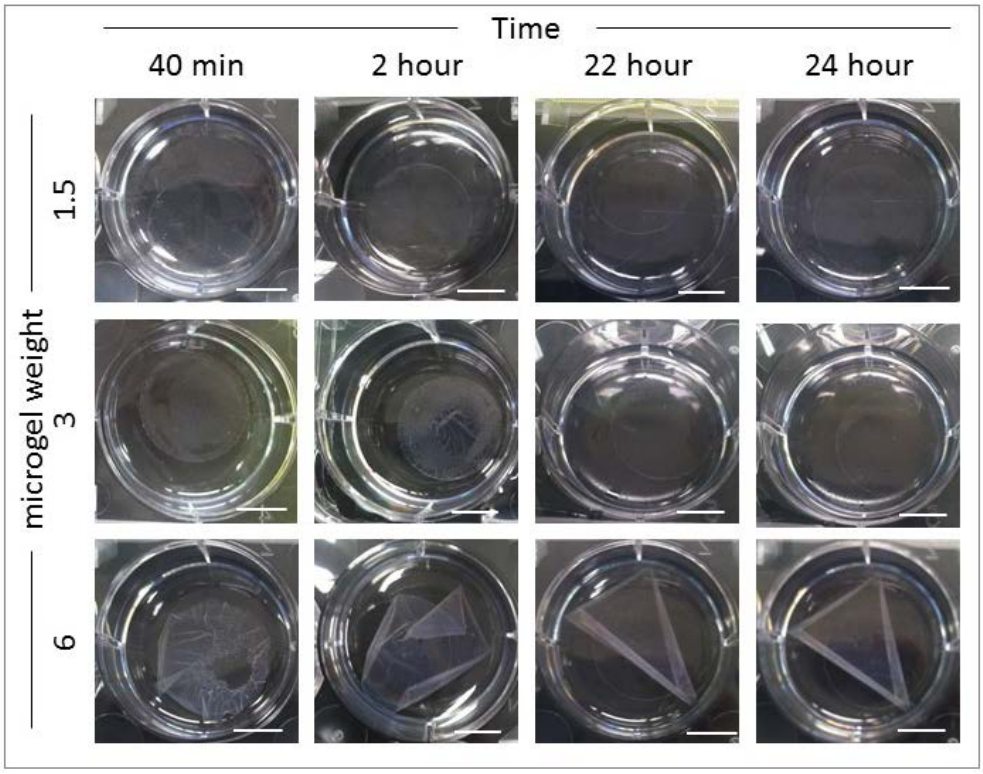

Figure S2. Characterization of film swelling dependence on film size. Microgel films of varied thickness were prepared on functionalized glass coverslips (22 mm diameter) by modulating the weight of polymer used during fabrication. Films were dried and then hydrated in 10 mM formate (pH 3.3) with 100 mM NaCl. Films were left on a shaker for 24 h to assess detachment. Scale bars represent 10 mm.

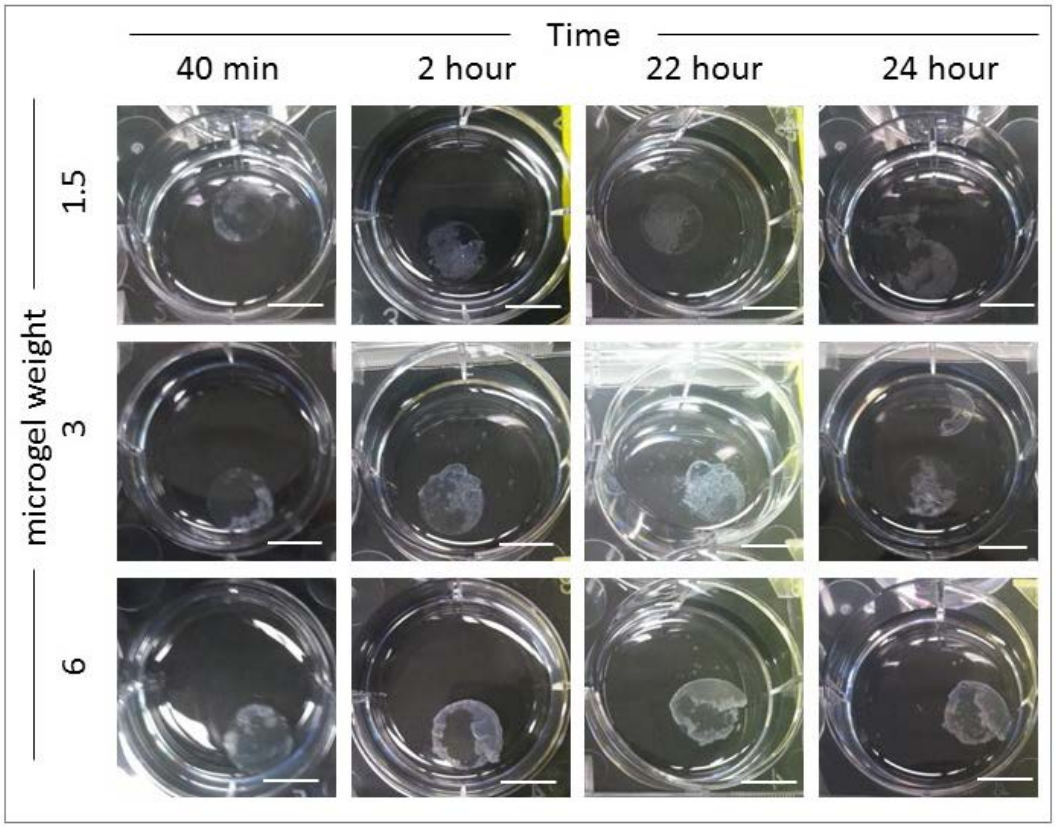

Figure S3. Characterization of film swelling dependency on film size. Microgel films of varied thickness were prepared on functionalized glass coverslips (12 mm diameter) by modulating the weight of polymer used during fabrication. Films were dried and then hydrated in 10 mM formate (pH 3.3) with 100 mM NaCl. Films were left on a shaker for 24 h after which detachment was assessed. Scale bars represent 10 mm.

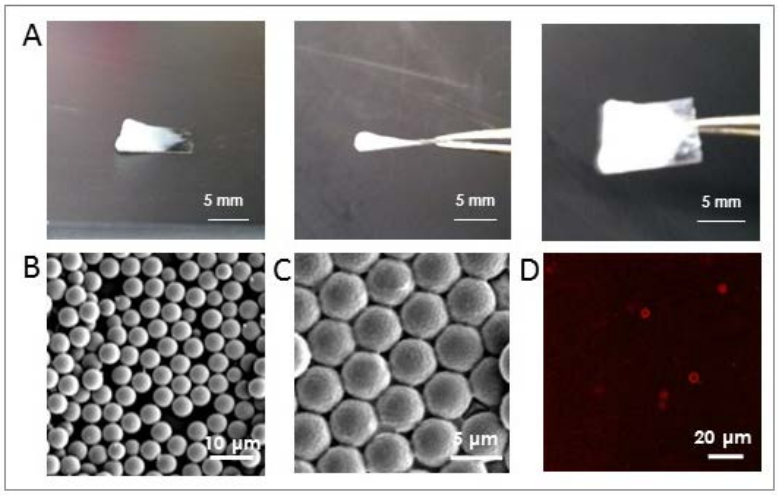

Figure S4. Visual characterization of films fabricated using the single-step fabrication technique. (A) Microgel wedges were prepared using the single-step fabrication technique by placing 0.40 mL of PEI suspended in PBS, 0.40 mL of 10mg/mL microgel suspended in PBS, and 0.80 mL of PBS in a well located in either the 1st or last column of a 24 well-plate during centrifugation. The single step fabrication can also be used to fabricate monolayers of (B) carboxyl-functionalized polystyrene beads and (C) raspberry-like particle (imaged via brightfield microscopy). (D) The single-step fabrication technique can also be used to prepare films/gels containing multiple building blocks, in this case Rho-B labeled microgels and carboxyl functionalized polystyrene beads (imaged via laser scanning confocal microscopy).

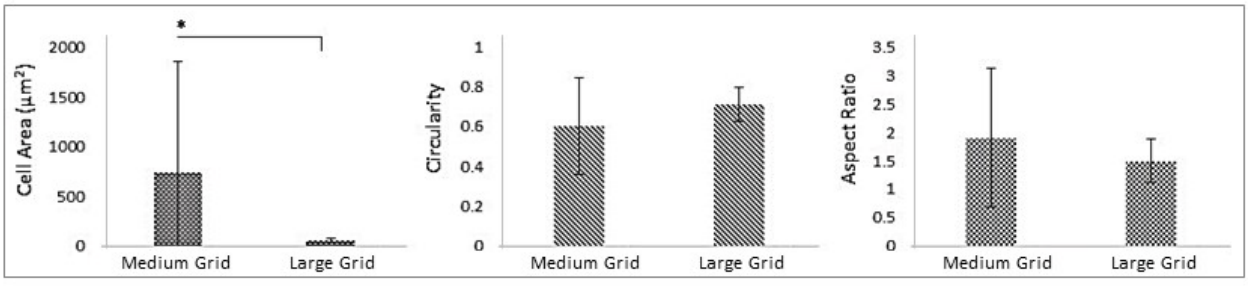

Figure S5. Fibroblast spreading on microgel films. A two-tailed unpaired p-test was performed to assess statistical significances (*= $p<0.01$).

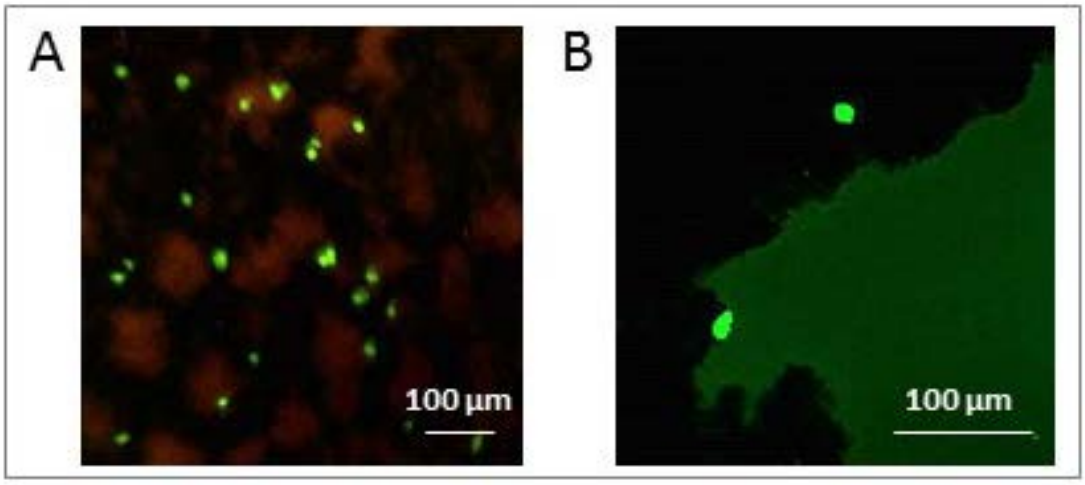

Figure S6. ATII adhesion behavior is influenced by film patterns. ATII cells were stained with CellTracker Green CMFDA to visualize the cell membrane. Cells were plated at a density of 5,000 cells/cm^2 on laterally patterned microgel films with either (A) 85 µm x 85 µm squares or (B) 283 µm x 283 µm.

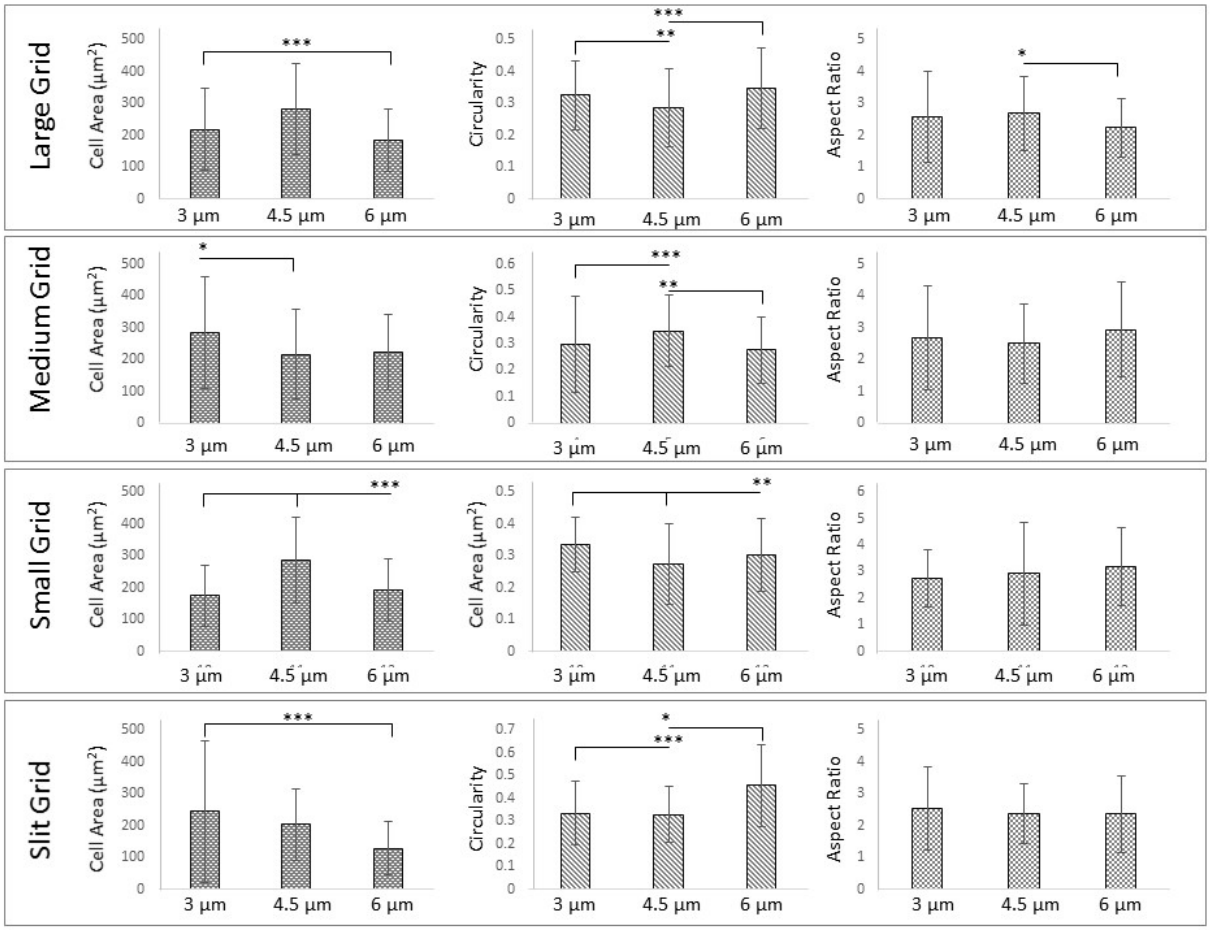

Figure S7. Fibroblast spreading on PS films. Comparison between fibroblast spreading responses on grid patterns with varied PS bead sizes. Statistical analysis was performed using the Kruskal-Wallis test with Dunn post-test. Cells were not expected to exhibit a Gaussian distribution in response to these conditions. All sample points were pooled together for statistical analysis (***= $p<0.001$, **= $p<0.01$, *= $p<0.05$).

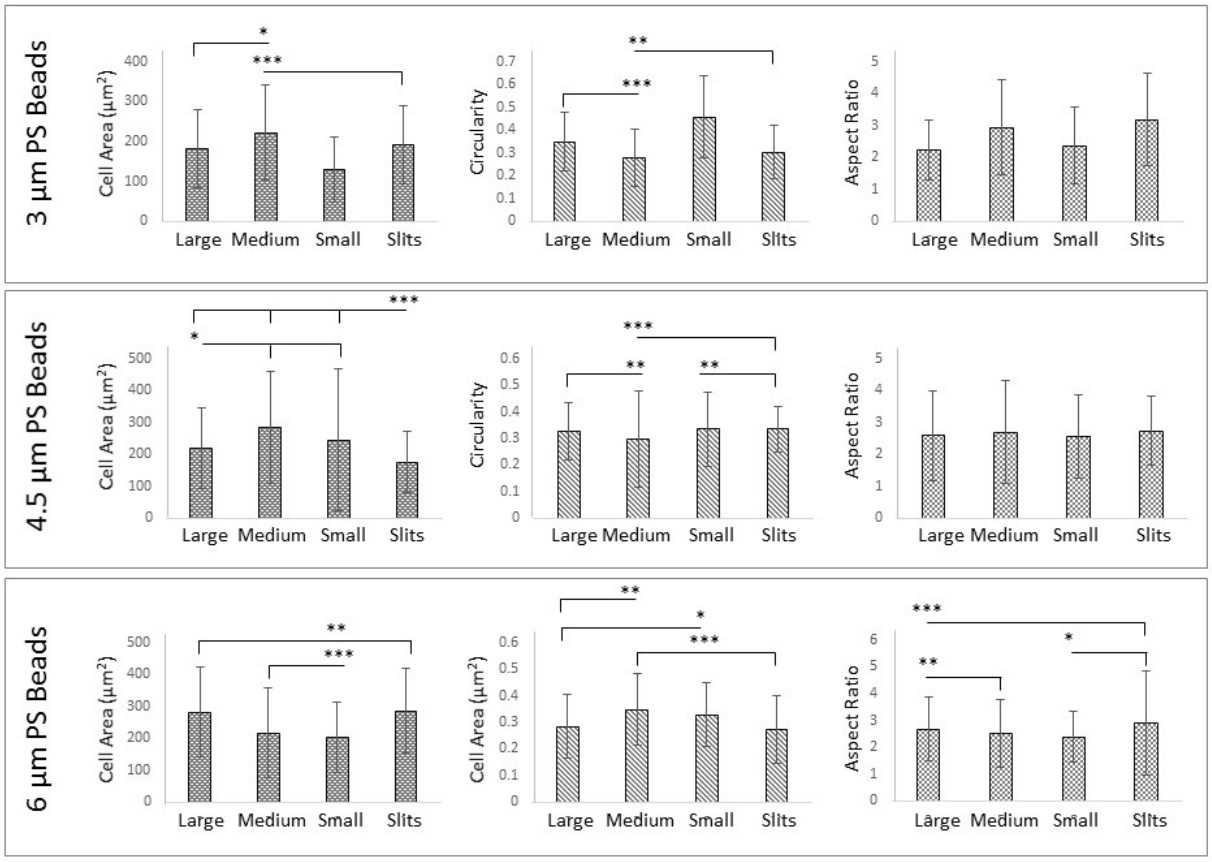

Figure S8. Fibroblasts on PS films. Comparison between fibroblast responses to different grid patterns at the same PS bead sizes. Statistical analysis was performed using the Kruskal-Wallis test with Dunn post-test. Cells were not expected to exhibit a Gaussian distribution in response to these conditions. All sample points were pooled together for statistical analysis (***= $p<0.001$, **= $p<0.01$, *= $p<0.05$).

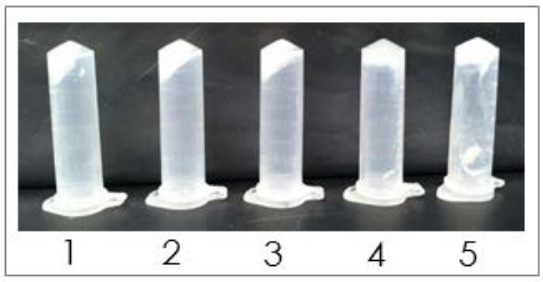

Figure S9. Development of bulk polyelectrolyte gels. Samples 1-3 are composed of the 4 mol-% BIS microgels and have been cross-linked with EDC/NHS at 20/50 mM, 2/5 mM, and 0.2/0.5 mM concentrations, respectively. Sample 4 contains a ULC gel and sample 5 is a mixture of 4 mol-% BIS microgels and ULC microgels.

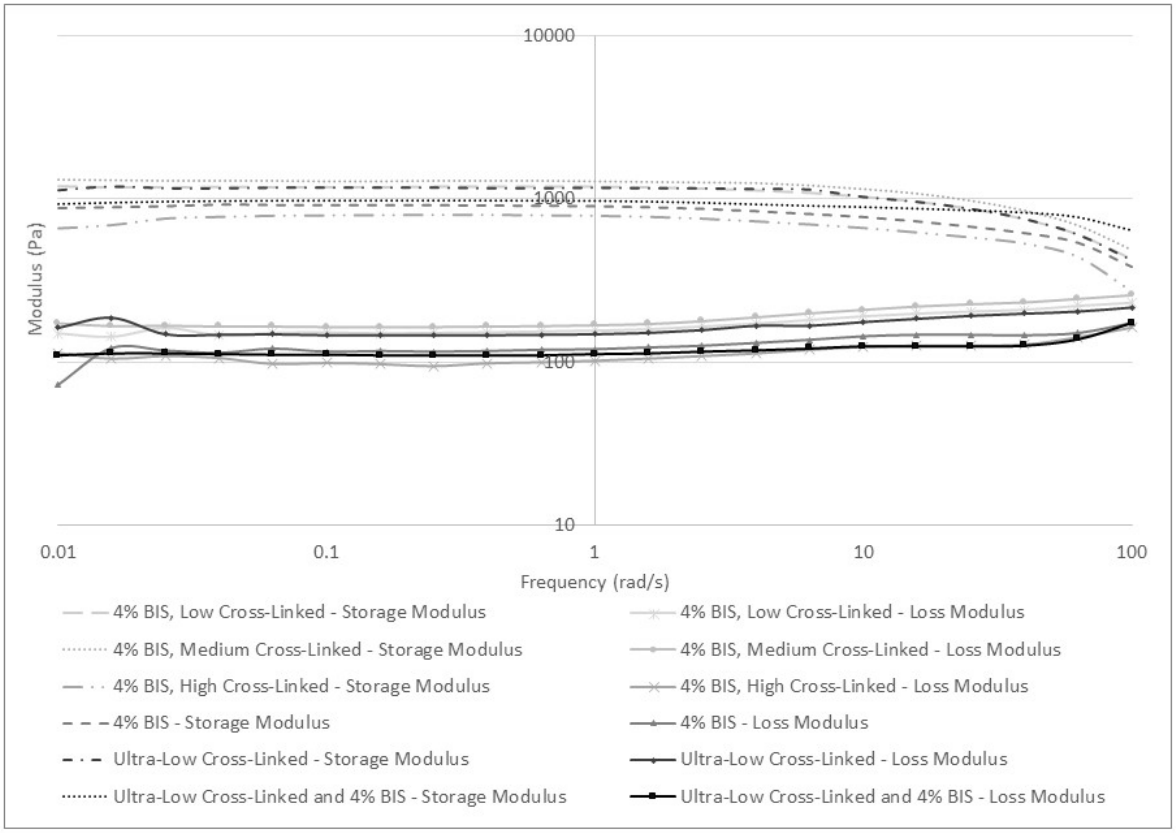

Figure S10. Rheological characterization of bulk polyelectrolyte gels. Strain sweeps were performed to identify a linear regime to perform frequency sweeps.

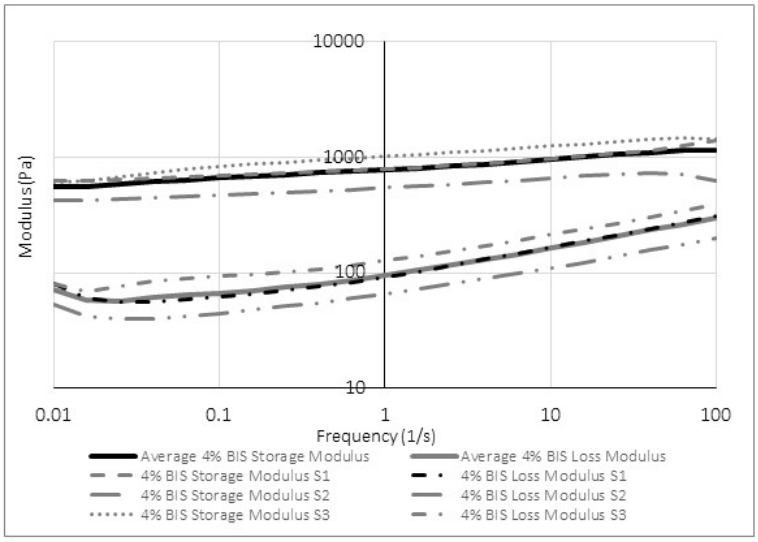

Figure S11. Rheological characterization of 4 mol-% BIS microgel bulk polyelectrolyte gel sample. The average of the three samples tested (S1, S2, and S3) is displayed by a solid line.

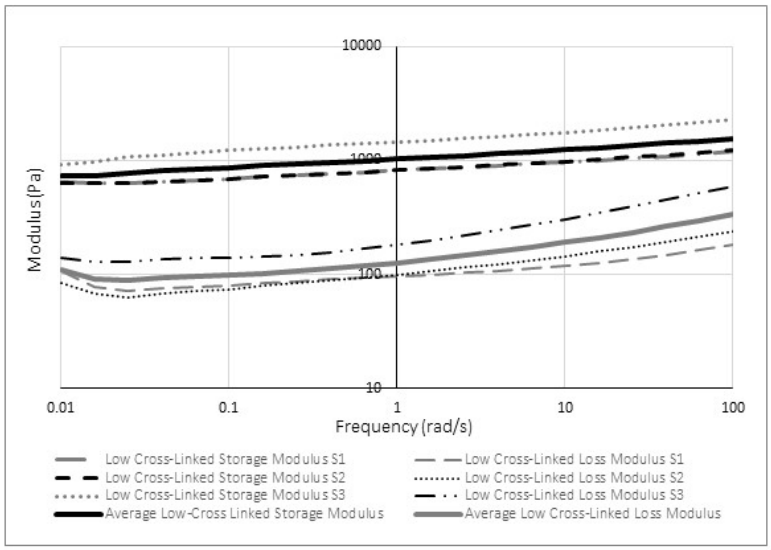

Figure S12. Rheological characterization of 4 mol-% BIS microgel bulk polyelectrolyte gel sample cross-linked with EDC/NHS 0.2/0.5 mM. The average of the three samples tested (S1, S2, and S3) is displayed by a solid line.

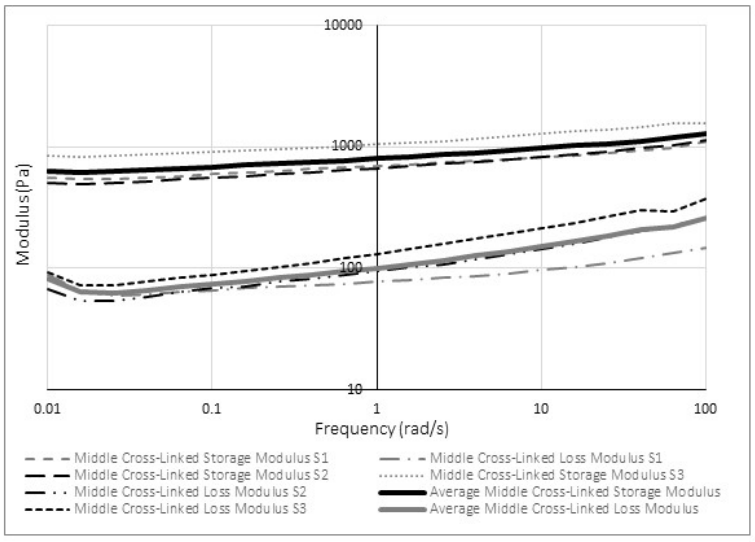

Figure S13. Rheological characterization of 4 mol-% BIS microgel bulk polyelectrolyte gel sample cross-linked with EDC/NHS 2/5 mM. The average of the three samples tested (S1, S2, and S3) is displayed by a solid line.

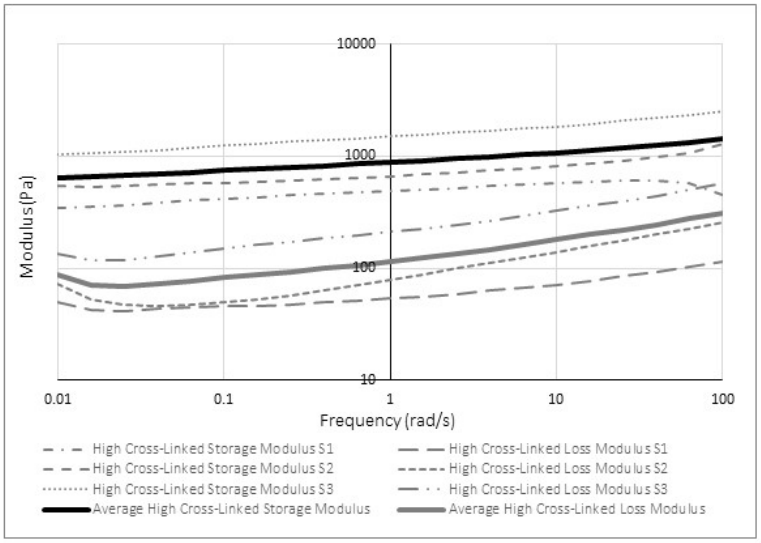

Figure S14. Rheological characterization of 4 mol-% BIS microgel bulk polyelectrolyte gel sample cross-linked with EDC/NHS 20/50 mM. The average of the three samples tested (S1, S2, and S3) is displayed by a solid line.

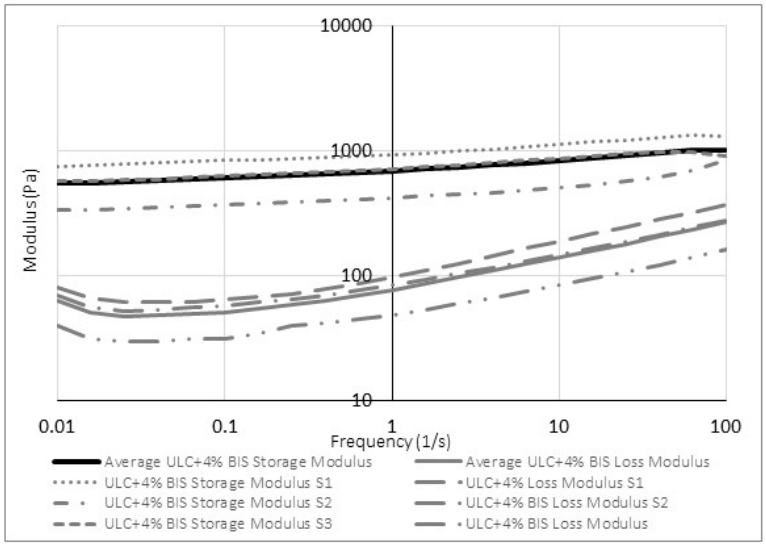

Figure S15. Rheological characterization of 50/50 mixture of ULC microgels and 4% BIS microgels in a bulk polyelectrolyte gel sample. The average of the three samples tested (S1, S2, and S3) is displayed by a solid line.